Volume 1 | Number 1 | Jan 2013 | Pages 1–100

PCCP

Physical Chemistry Chemical Physics
www.rsc.org/pccp

ROYAL SOCIETY OF CHEMISTRY

ROYAL SOCIETY OF CHEMISTRY

www.rsc.org/pccp

ARTICLE TYPE

The Study into the Extracted Ion Number for NASICON Structured Na₃V₂(PO₄)₃ in Sodium-ion Batteries

Weixin Song, Zhengping Wu, Jun Chen, Kaili Huangfu, Xiaowen Wang, Yaliang Huang and Xiaobo Ji*

Excellent C-rate and cycling performances with a high specific capacity of 117.6 mAhg⁻¹ have been achieved on NASICON-structure Na₃V₂(PO₄)₃ sodium-ion batteries. Two different Na sites namely Na(1) and Na(2) site are reported in the open three-dimensional framework, of which the ions at Na(2) sites should be mainly responsible for the electrochemical properties. It is vitally important and ₁₀ interesting to find that there are two kinds of possible ions occupations of Na ions in Na₃V₂(PO₄)₃ and the investigation of ion-extraction number is firstly explored by discussing ions occupations with the help of first-principles calculations. The ion occupation of 0.75 for all Na sites is suitable for the configuration of [Na₃V₂(PO₄)₃]₂, and the two-step extraction process accompanied by structure reorganization is capable to account for the theoretical capacity of Na₃V₂(PO₄)₃.

15

1. Introduction

Better-performing energy storage systems have been driven into great concerns in order to get breakthroughs to promote the usage of electricity as a result of the increasing environmental pollution ₂₀ and gradual depletion of oil resources, such as the lithium-ion battery (LIB) which has been undergone intensively research to enhance the electrochemical properties[1, 2]. However, the existing lithium-ion battery technologies, especially available for large-scale energy storage have exhibited many shortcomings in cost, ₂₅ material stability issues, cycling and safe performances [3, 4]. Additionally, the amount of Li resources in the earth which are not sufficient to satisfy the increasing demands on LIB, should also arouse the public concerns since a expanding need of LIB in portable electronics and large-scale applications, in particular, ₃₀ electric vehicles (EVs)[1, 2]. As a result of the abundance and low cost of Na, as well as its similarly chemical properties as compared with Li, sodium-ion battery (SIB) also has been constructed based on the fundamental principles of LIB, utilizing the chemical potential difference of Na ions between two ₃₅ electrodes (anode and cathode) to create a voltage on a cell and charge or discharge by the shuttling Na ions between two electrodes[5]. Reasonably, the Na-based electrode would be considered capable to play a vital role in the electrochemical performances of SIB, while the unexplored opportunities towards ₄₀ Na-based battery systems could also be of great significance for the development.

NASICON (Na superior conductor)-structure compounds feature a highly covalent three-dimensional framework that generates large interstitial spaces through which sodium ions can ₄₅ diffuse[6, 7], such as Na₃M₂(PO₄)₃ (M=Ti, Fe, V)[4, 8-13] and Na₃V₂(PO₄)₂F₃[14-16]. NASICON-type Na₃V₂(PO4)₃ (NVP) has been investigated recently as a mainly prospective cathode material for sodium ion batteries[17], and the composition of phosphate-based Na-insertion hosts is advantageous due to the ₅₀ strong covalent (PO₄)³⁻ units that could provide structural stability even at high charge states, and the enhanced thermal safety concerns unlike commercial Li-insertion oxide hosts[9, 18-21]. NVP

displays two potential plateaus at 3.4 V and 1.6 V vs. Na⁺/Na, related to the V³⁺/V⁴⁺ and V²⁺/V³⁺ redox couples, and these two ₅₅ reaction voltages correspond to a specific capacity of 117.6 and 50 mAhg⁻¹ for the high and low voltage zones, respectively. Moreover, the voltage plateau located at 3.4 V is relatively higher than that of other cathode materials in sodium-ion batteries[22-27] which is capable to demonstrate its suitability as a cathode, while ₆₀ the separated lower potential at 1.6 V could also make it possible to be anode[4, 28]. Moreover, Lim et al. have correlated these two potential plateaus with the energies calculated for different Na distributions in the phase[29], and the transported Na ion number should be determined by the applied voltage range which can ₆₅ directly influence the capacity performance[15, 30]. The NVP crystal shows that the octahedral VO₆ interlinks via corners with tetrahedral PO₄ to establish the polyanion [V₂(PO₄)₃] units in the c-axis direction which were interconnected through PO₄ to the same neighboring units, and each primitive cell of NVP contains ₇₀ six formula units built up from [V₂(PO₄)₃] framework anion and two different oxygen environment sodium atoms, of which the first one is six fold coordination [Na(1)] and the other is eight fold coordination [Na(2)]. Four cations could be hosted in the voids/channels per formula unit of [V₂(PO₄)₃] if all the Na sites ₇₅ could be occupied, presenting a theoretical capacity of 235 mAhg⁻¹[9]. A two-phase reaction was considered to generate from Na₃V₂(PO₄)₃ to NaV₂(PO₄)₃ with the sodium content in Na(2) site going, while the Na(1) site remains totally occupied with one Na ion to produce a theoretical capacity of 117.6 mAhg⁻¹ [9, 29]. ₈₀ Thereby, the extracted ions from a specialized Na site can produce great influences on the electrochemical performances of the battery. However, there has been reported that the ion occupation in two crystallographic sites is rather than an integer[29], illuminating that it might be an interesting work to ₈₅ explore the transported number of sodium ions in a NVP unit between two electrodes.

Thus, a NVP/NaClO₄/Na sodium-ion battery was constructed to explore the ion transportation mechanism, using NVP synthesized by a solution-based carbothermal reduction method ₉₀ (S-CTR). The electrode material here used shows better performances than that prepared by carbothermal reduction

method (CTR), which was authenticated by the compared electrochemical behaviors of NVP/LiPF$_6$/Li hybrid-ion batteries from our previous works[30]. Furthermore, the auxiliary first-principles calculations were employed to investigate the structural characteristics as well as the possible number of extracted ions from NVP.

2. Experimental Section

NVP was prepared by solution-based carbothermal reduction method (S-CTR) using a solvation-based precursor. Stoichiometric amounts of analytical purity Na$_2$CO$_3$, NH$_4$H$_2$PO$_4$, V$_2$O$_5$ and acetylene black powders (5 wt.% excess acetylene black would be used as conductive agent while these as reducer for the reaction should match the stoichiometric ration) were mixed and stirring in distilled water and dried under 50 ºC by forced-air drying. The precursor was ground and preheated at 350 ºC in flow argon for 4h, and reground before being re-fired at 650 ºC in argon atmosphere for 8h.

The crystallographic structure of the as prepared material was studied by X-ray powder diffraction (XRD) using a Bruker D8 diffractometer with monochromatic Cu Kα radiation (λ=1.5406 Å), and the diffraction data was recorded in the 2θ range of 10–60 º with a scan rate of 8 º/min. The infrared (IR) spectra was obtained using an FT-IR Spectrometer (Jasco, FT/IR-4100, Japan) under transmission mode based on the KBr pellet method in the range of 500-2000 cm^{-1}. The particle morphology of the composite was investigated by a FEI Quanta 200 scanning electron microscopy (SEM). The thermogravimetric analysis (TG) of the samples was carried on a Diamond TG thermo-analyzer under oxygen atmosphere with a heating rate of 10 ºC/min.

NVP/NaClO4/Na system was employed into a sodium-ion battery to be investigated in this work. The cathode electrode was fabricated with the active material, acetylene black, and binder (Polyvinylidene Fluoride, PVDF) in a weight ratio of 8:1:1 by using NMP as solvent and an aluminum foil as current collector (the loading material is about 4.5 mg/cm^2), followed by drying in vacuum at 110 ºC for 24 h. The R2016 coin cell was assembled in an argon-filled glove box using sodium foil as anode, Celgard 2500 membrane as separator. The electrolyte was 1 M NaClO$_4$ dissolved in polycarbonate (PC).

Cyclic voltammetry (CV) and galvanostatic charge/discharge cycling tests were carried out in a setting voltage range by using an electrochemical workstation (CHI660C) and a CT2001A LAND battery tester, respectively. All electrochemical tests were carried out at room temperature.

All calculations on Na$_3$V$_2$(PO$_4$)$_3$ were performed with the spin-polarized Generalized Gradient Approximation (GGA) using the Perdew–Burke–Ernzerhof (PBE) exchange-correlation parameterization to Density Functional Theory (DFT) using CASTEP program. A plane-wave basis with a kinetic energy cutoff of 330 eV was used, and size of standard grid was 1.5. BFGS optimization method was used and the geometry optimization parameters of total energy convergence, max ionic force, max ionic displacement and max stress component tolerance were 0.2×10^{-4} eV/atom, 0.5×10^{-1} eV/ Å, 0.2×10^{-2} Å and 0.1GPa respectively. The electronic convergence thresholds parameters of total energy and eigen-energy were 0.2×10^{-5} eV and 0.5638×10^{-6} eV. All calculations were conducted in a unit cell of [Na$_3$V$_2$(PO$_4$)$_3$]$_2$.
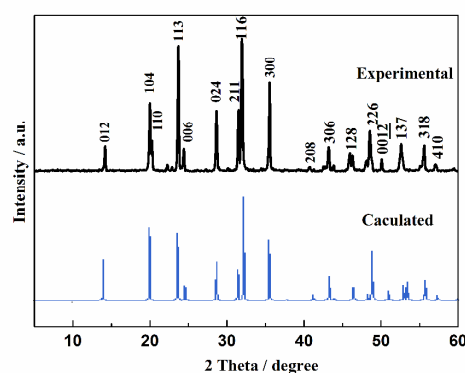
3. Results and discussion

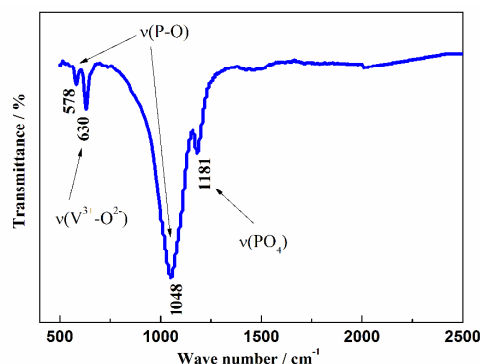**Fig. 1** XRD patterns of the as-prepared material.

Fig. 2 FI-IR spectrum of NVP recorded in the range of 500—2000 wave numbers.

Fig. 1 shows the XRD of NVP prepared by S-CTR at 650°C as well as the calculated XRD patterns. All the diffraction peaks are well-indexed to the R-3c space group under the rhombohedral NASICON structure with a=b=8.72 Å and c=21.764 Å, which are also in good agreement with previous reports [4, 6, 10]. Moreover, these experimental results are also well consistent with the calculated values based on the first-principles calculations. At the same time, the sharp peaks from the experiment which match the simulated results very well including the peak positions and intensities, could indicate a good crystallinity for the as-prepared material [10]. Clearly, a pure NVP was successfully obtained by this developed S-CTR method on account of the solution-based admixture which has improved the contacted effects among the particles. However, the characteristic diffraction peaks of graphite are not observed from the experimental XRD patterns, illustrating that the residual carbon in this product is in an amorphous state [31]. The FT-IR analysis of S-CTR NVP displayed in Fig. 2 agrees well with the previous works [29, 30], from which the bands could illuminate a fine crystallization due to the obviously appeared peaks. The bands at 578 and 1048 cm^{-1} suggest the presence of P-O bonds of PO$_4$ tetrahedra, and the vibration from V^{3+}-O^{2-} bonds in isolated VO$_6$ octahedra is detected at 630 cm^{-1}. Moreover, the infrared bands in the range of 1150–1250 cm^{-1} can be attributed to the stretching vibration of terminal PO$_4$ units[32]. While no bands corresponding to the occurrence of V^{5+} and V^{5+} in the prepared material have come out, this demonstrates that the V^{5+} in V$_2$O$_5$ has been reduced to V^{3+} in NVP and Na$_3$V$_2$(PO$_4$)$_3$ is more favorable to be synthesized as a result of the stable oxidation state of V^{3+} compared to the relatively unstable state of V^{2+} in Na$_4$V$_2$(PO$_4$)$_3$.
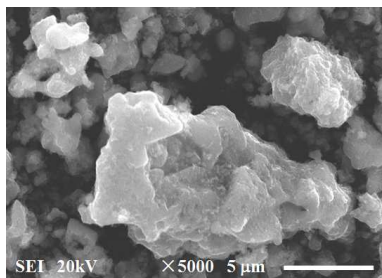
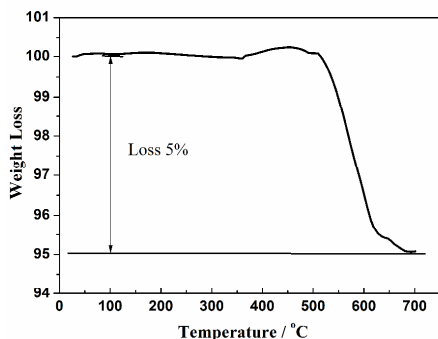**Fig. 3** SEM images of the as-prepared NVP

Fig. 4 TG curve of NVP in air atmosphere.

The morphology and surface structure of the S-CTR NVP were characterized by SEM and the images are shown in Fig. 3. It could be observed that the synthesized material has presented a rugged surface with a few pores. This structure could be beneficial for the ions to transport or facilitate the ion diffusion from/into the three-dimensional NASICON structure[15], to some extent. As known to all, the redundant carbon in the prepared particles should be responsible for the hindering effects on particles growth during the synthesized process at a high temperature. Thus, the formation of NVP particles in this work might have been influenced by these carbon source evaluated as 5% according to the TG curves in Fig. 4, and the weight increase around 400 °C could be attributed to the oxidation of V^{3+} in NVP. Moreover, the existed carbon content could be favorable to improve the conductivity of the electrode material.
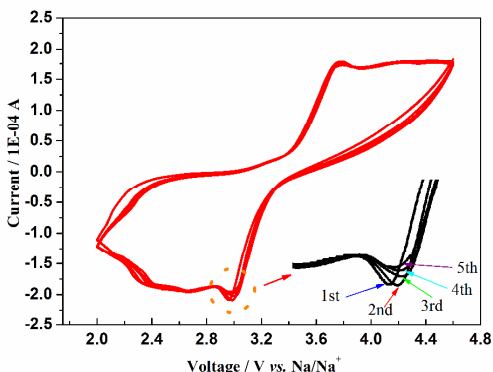

Fig. 5 The first five CV cycles of S-CTR NVP at 0.5 mV/s between 2—4.6 V vs. Na/Na$^+$, the inset shows the magnified image located around the reduction peaks.

The CV curves of the first five cycles for the S-CTR NVP sodium-ion battery without pre-cycling are displayed in Fig. 5 in a voltage range of 2—4.6 V vs. Na/Na$^+$ at 0.5 mV/s, the similar curves of which could indicate a fine cycling stability and reversibility of NVP electrode[33]. Additionally, the oxidation (Na extraction) and reduction (Na insertion) peaks are located at 3.7

and 3 V, respectively, while the unobvious redox couple around 2.3 V could be considered helpful to complete the extraction/insertion of Na ions. In situ XRD and ICP (Inductively Coupled Plasma) investigation have been used to demonstrate the formation of $NaV_2(PO_4)_3$ when the sodium ions were chemically extracted from $Na_3V_2(PO_4)_3$ during charging process[10]. In addition, Ex-situ XPS (X-ray photoelectron spectroscopy) studies were carried out to examine the Na ion insertion/extraction mechanism from which the oxidation and reduction of vanadium from V^{3+} to V^{4+} and back to V^{3+} were found out accompanied with migration of two Na ions[4]. Thus, a redox reaction to realize V^{3+}/V^{4+} transformation with the transport of two Na ions is expected in this specific voltage window. Meanwhile, the reduced peaks were found to shift towards higher potential gradually during cycling while the oxidation peaks seemed not shifted leaving the hysteresis between the couple of redox peaks to decrease, which could demonstrate the good reversible capability of the material with the electrode undergoing minor structure rearrangement[15].
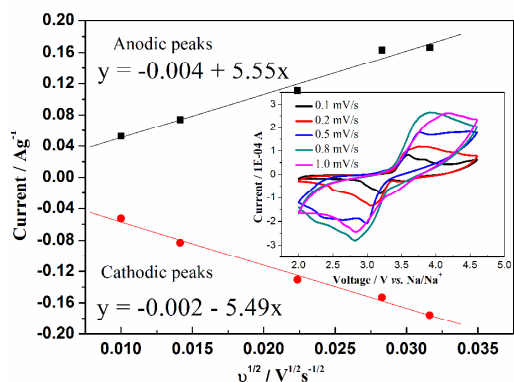

Fig. 6 The corresponding relationship between the square root of the scan rate $v^{1/2}$ and peak current i_p, the inset shows CV curves at different scan rates of S-CTR NVP in a voltage range of 2–4.6 V vs. Na$^+$/Na.

CV tests of the sodium-ion battery with S-CTR NVP at 0.1, 0.2, 0.5, 0.8 and 1 mV/s in a voltage range of 2—4.6 V vs. Na$^+$/Na, are displayed in the inset of Fig. 6, from which the increased cathode-anode peak differences with the increasing of scan rates indicate an enlarged irreversibility at high current densities. Meanwhile, the liner relationship between the peak current i_p and the square root of the scan rate $v^{1/2}$ as presented in Fig. 6, indicate a diffusion-controllable process for the whole electrode reaction, and the corresponding Na ions diffusion D_{Na+} is capable to be calculated by Randles-Sevcik equation (Equation 1)[30, 34-36] which describes the relationship between the peak current i_p and the square root of the scan rate $v^{1/2}$.

$$i_p/m = 0.4463(F^3/RT)^{1/2}n^{3/2}AD^{1/2}Cv^{1/2} \tag{1}$$

where m is the mass of active cathode material, F is the Faraday constant, R is the gas constant, T is the absolute temperature, n is the number of electrons in reaction (n = 2), A (0.78 m^2)is the effective contact area between electrode and electrolyte used for simplicity[35], D is the diffusion constant and C (2.35×10^{-3} mol/cm^3) is the concentration of Na ion in the cathode calculated on the crystallographic parameter of NVP. Herein, the S-CTR NVP could produce an anodic and cathodic D_{Na+} value of 1.05×10^{-11} cm^2/s and 1.03×10^{-11} cm^2/s, respectively, and it's clear that the D_{Na+} value of NVP SIB is much lower than that of NVP-cathode hybrid-ion battery we previously reported[30] which should be

attributed to the heavier mass and larger volume for sodium ions in transportation. It is another way to again prove that the existence of a predominately lithium-ion diffusion in mixed Na/Li transportation for NVP hybrid-ion battery, results in the high D value, otherwise, the value might be lower as a result of the effects from Na ions.
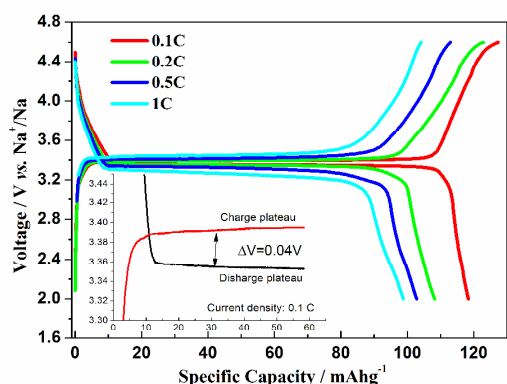

Fig. 7 Initial charge/discharge profiles of S-CTR NVP sodium-ion battery at 0.1C, 0.2C, 0.5C and 1C, respectively, in a voltage range of 2–4.6 V vs. Na$^+$/Na. Inset is the polarization of NVP electrode at 0.1C.

**Table 1.** Experimental results for NVP sodium-ion battery

	This work	Ref[33]	Ref[4]	Ref[10]	Ref[10]	Ref[10]	Ref[10]	Ref[10]
Electrolyte	NaClO$_4$	NaClO$_4$	NaClO$_4$	NaClO$_4$	NaBF$_4$	NaPF$_6$	NaFSI	NaFSI
Solvent	PC	PC	EC/PC	PC	PC	EC/DEC	EC/DEC	PC
Initial C (mAhg^{-1})	117.6 (0.1 C)	93 (0.05 C)	116 (0.1 C)	82.6 (0.1 C)	-	-	-	108.5 (0.1 C)
Coulombic efficiency	94.4%	94.2%	~96.7%	82%	94.4%	96.3%	98%	98.2%

Fig. 7 shows the charge/discharge curves of the NVP/Na cell at different current densities of 0.1C, 0.2C, 0.5C and 1C (note that 1C refers to two Na extraction from the NVP per formula unit in 1h.), with the corresponding specific capacities of 117.6, 111, 104 and 100 mAhg^{-1}, respectively, in a voltage range of 2–4.6 V vs. Na$^+$/Na. The corresponding coulombic efficiencies of the initial cycle for different current rates are 94.4%, 92%, 92.8% and 97%, respectively, of which the high efficiency even for the large rate should be attributed to the special surface structure of S-CTR NVP. Though the variety of Na-based electrolyte and solvent might have played an important role in the electrochemical properties of the SIB, the presented performances in this work are comparable with reported work as listed in Table. 1. The obvious flat voltage plateaus are almost stabled at 3.39 V for charge and 3.36 V for discharge with a polarization of 0.04 V (as shown in the inset of Fig. 7) of which this lower value compared with Jian et al.'s work (0.07 V), could imply a good electronic and ionic conduction[29, 33].
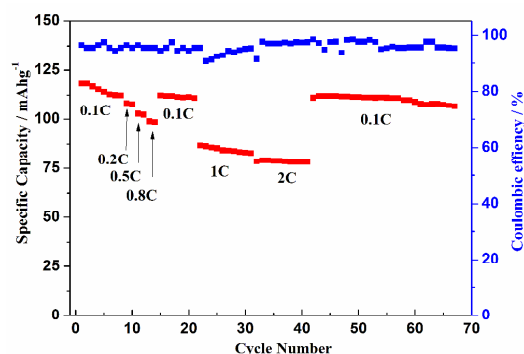
Fig. 8 C-rates and cycling performances for NVP sodium-ion battery.

The C-rate and cycling performances of the S-CTR NVP SIB are shown in Fig. 8. A desirable property of a high capacity ca. 80 mAhg^{-1} with a coulombic efficiency ca. 98% are presented at a high current density of 2C undergoing 30 cycles, which is comparable with the results reported[9]. Furthermore, it could be found that NVP retained a capacity ca. 109 mAhg^{-1} (91% retention to the initial capacity) after 68 cycles when re-tested at 0.1C, which would indicate NVP prepared by S-CTR method to be able to be used as a promising electrode material in sodium-ion battery.
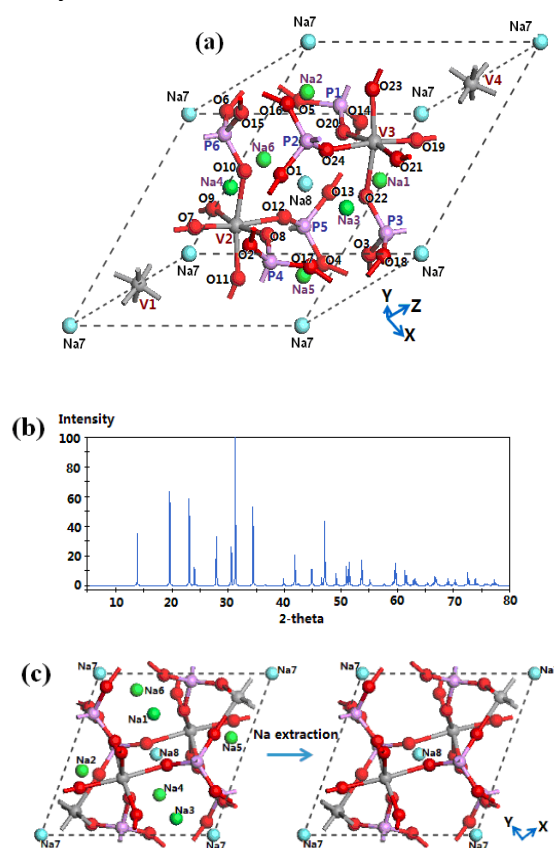
Fig. 9 (a) Schematic representation of a refined NVP structure, and (b) the corresponding simulated XRD of the refined NVP, and (c) the scheme of Na extraction in charging. Na1, Na2, Na3, Na4, Na5, Na6 occupied the Na(2) sites and Na7, Na8 occupied Na(1) site in NVP.

Table 2. Atom coordinates of $Na_3V_2(PO_4)_3$.

Site	Element	Wyckoff Symbol	Symmetry	x	y	z	Occupation
O1	O	36f	1	0.01714	0.20172	0.19119	1
O2	O	36f	1	0.18532	0.16658	0.08488	1
P1	P	18e	.2	0.29683	0	1/4	1
Na1	Na	18e	.2	0.63747	0	1/4	0.750
V1	V	12c	3.	0	0	0.14679	1
Na2	Na	6b	-3.	0	0	0	0.750

Table 3. Atom coordinates of $Na_2V_2(PO_4)_3$.

Site	Element	Wyckoff Symbol	Symmetry	x	y	z	Occupation
O1	O	36f	1	0.01714	0.20172	0.19119	1
O2	O	36f	1	0.18532	0.16658	0.08488	1
P1	P	18e	.2	0.29683	0	1/4	1
Na1	Na	18e	.2	0.63747	0	1/4	0.500
V1	V	12c	3.	0	0	0.14679	1
Na2	Na	6b	-3.	0	0	0	0.500

Notably, the extracted ion number from the cathode would determine the exhibited performances particularly for the specific capacity. The theoretical capacity of NVP is claimed to have a value of 117.6 $mAhg^{-1}$ with the migration of two Na ions in the redox reaction for each $Na_3V_2(PO_4)_3$, and the current investigations have presented the approximately theoretical values for NVP electrode[4, 10]. To explore the ion number which could extract from per NVP unit, the first-principles calculations were employed to elucidate the mechanism of the structural evolution and the electrochemical behaviours of the Na ions in NVP SIB. Here, the atom coordinates of NVP originated from *The Landolt-Börnstein Database in Springer Materials* (Table. 2 and 3) were utilized to construct the computed model in this work while to the best of our knowledge, only few literatures have given these information[6]. The schematic representation of the refined NVP crystal structure is presented in Fig. 9(a) with corresponding simulated XRD patterns as shown in Fig. 9(b). The ions occupied different Na sites are notated with various numbers where the sodium ions at Na(2) site are marked from Na1 to Na6 and these at Na(1) site are from Na7 to Na8, and they are distinguished by the different oxygen surroundings which could play a significant role in the ion extraction process. Furthermore, the simulations as well as the specific notations can be considered reasonable as the consistence with the results in previous literatures [4, 6, 10].

Table 4. Bond population and length for NVP and ion-extracted NVP.

Bond	Optimized cell		Optimized 6 Na extracted cell	
	Population	Length(Å)	Population	Length(Å)
O-Na(1~6)	-0.04, -0.02, 0.05	—	—	—
O-Na(7~8)	0.09, 0.1	2.547~2.548	-0.02	2.516~2.517
O-V	0.3, 0.36	2.028~2.156	0.36, 0.40	1.893~1.985

The simulated unit cell of $[Na_3V_2(PO_4)_3]_2$ was constituted according to the atom coordinates listed in Table. 2 and Table. 3. However, two kinds of Na occupations have been reported, one of which presents a same Na occupation of 0.75 for Na(1) and Na(2) sites when referred to *Gopalakrishnan's* conclusions[6], and the other one coming from *Jang et al.*[29] shows an occupation that 1 for Na(1) and 0.67 for Na(2) sites. Based on the structural characteristics, all the DFT calculation results are listed in Table S1~S7, and the bond populations of Na-O have been recorded in Table 4. The values for Na(2) sites are found smaller than that for Na(1) sites, which could illuminate that the ions at Na(2) sites would be easier to extract at an early charging stage[16, 34]. *Lim et al.*[29] have reported their conclusions that the ions occupying Na(1) site have the occupancy of 1 and those occupy Na(2) sites have the occupancy of 0.67 in the crystal structure of $Na_3V_2(PO_4)_3$. This kind of distribution is capable to explain that nearly 2.01 ions would extract from $Na_3V_2(PO_4)_3$ to produce a specific capacity approaching 117.6 $mAhg^{-1}$ when the ions at Na(2) sites marked as Na1~Na6 have been considered to totally migrate out from $[Na_3V_2(PO_4)_3]_2$. However, because the six ions at Na(2) sites with an occupation of 0.67 are equal to 4.02 ions and the ions at Na(1) sites with an occupation of 1 correspond to 2 Na ions, thus this distribution of ion occupation would contribute to a unit of $[Na_{3.01}V_2(PO_4)_3]_2$ which only approximate the configuration of $[Na_3V_2(PO_4)_3]_2$ in calculation.

Table 5. Compared lattice parameters for NVP and ion-extracted NVP by optimization.

Parameter	Experimental	Optimized cell	Optimized extracted cell
a	8.856794	9.051504	8.863846
b	8.856961	9.051540	8.864116
c	8.856965	9.052335	8.863746
α	59.219416	59.766075	57.520805
β	59.219703	59.759281	57.519083
γ	59.219963	59.766965	57.514279
$V(Å^3)$	482.549328	521.622651	464.339561

However, a fine unit of $[Na_3V_2(PO_4)_3]_2$ can be generated by adopting the values given in Table. 2 in which the ion occupations for all the Na ions have been defined to be 0.75. In that case, a total of 4.5 ions are indicated to occupy Na(2) sites and 1.5 ions occupy Na(1) sites in this simulated unit, and equivalently, there are 2.25 Na ions from Na(2) sites per formula of $[Na_3V_2(PO_4)_3]$ capable to extract in charging process. When the six Na(2)-site ions have migrated out totally, the extraction of Na ions from Na(1) sites would be still considered to be limited as a consequence of the decrease of bond length with a produced strong inductive effect, though the bond populations of Na-O were found to decrease synchronously. The bond lengths of O-V have been also observed to decline with the almost stable bond populations as displayed in Table 4, which should be attributed to the contraction of octahedral VO_6 when the vanadium has been oxidized accompanied with ion extraction, leading to the decrease of crystal lattices, as well. The lattice parameters of a unit cell $Na_3V_2(PO_4)_3$ (R-3c space group) before and after ion extraction are recorded in Table 5 when the simulating models have been optimized by DFT calculations. Based on the calculated results, the variation of lattice parameters and volume change from $Na_3V_2(PO_4)_3$ to $Na_{0.75}V_2(PO_4)_3$ are ca. 2% and 10%, respectively, which are comparable when $Na_3V_2(PO_4)_3$ turned into $NaV_2(PO_4)_3$ with a volume change of near 8.3%[10]. Moreover, according to Table S5 and S6, the total charge number of vanadium was found obviously increased from 3.21 to 5.3 from $Na_3V_2(PO_4)_3$ to $Na_{0.75}V_2(PO_4)_3$, from which this change of a non-integer also could illuminate that the two V(III) in NVP were oxidized to V(IV/V) on account of the more than two extracted ions in calculation. Additionally, the charges of the left two sodium ions denoted as Na7 and Na8 at Na(1) site are also increased to make

the ions more difficult to migrate out from the NASICON structure due to the stronger bond force between O and Na.

However, if the ion occupation of 0.75 for all Na ions in NVP is suitable, the theoretical capacity would be corrected as 131 mAhg^{-1} by employing Faraday's Law (C = 26.8n/M Ah/g, where C is the theoretical capacity of the active material, n is the number of electrons in reaction and M is the relative molecular mass). To the best of our knowledge, this theoretical value is not accepted and consistent with the experimental results[4, 10, 33] when all the ions at Na(2) sites have been assumed to be extracted totally by one step according to the above DFT calculation. While in this paper, a two-step ion extraction accompanied by the structure reorganization of NVP was proposed to explain the electrochemical behaviours of NVP. Referred to the literatures towards to the ion occupations of Na ions in a de-inserted $Na_2V_2(PO_4)_3$ phase, the ion occupation was found to changed to be 0.5 for ions at both Na(1) and Na(2) sites (shown in Table. 3). So the extraction of the first ion from NVP might be reasonable beginning from both Na(1) and Na(2) sites, corresponding to an phase transformation from $[Na_3V_2(PO_4)_3]_2$ (occupation of 0.75) to $[Na_2V_2(PO_4)_3]_2$ (occupation of 0. 5) with 1.5 ions extracting from Na(2) sites and 0.5 ion from Na(1) sites. During this process, it is inevitable to follow a structural reorganization of the $[Na_2V_2(PO_4)_3]_2$ as the ions configuration and chemical bonds have altered. This reorganization should have an prominent effect on the rearrangement of ions occupations with respect to the left ions in $[Na_2V_2(PO_4)_3]_2$, in order to make the ion extraction energetically favourable to form a relatively stable configuration $[NaV_2(PO_4)_3]_2$. Then the $[Na_2V_2(PO_4)_3]_2$ with three Na(2)-site and one Na(1)-site ions would prefer to contribute two ions extraction from Na(2) sites, leading to the phase of $[NaV_2(PO_4)_3]_2$ with one Na(2)-site and one Na(1)-site ion. Therefore, it is suggested that the Na ion configuration of $NaV_2(PO_4)_3$ should involve two different kinds of components, half one from Na(1) site and the other half from Na(2) site. The whole ion-extraction process of $Na_3V_2(PO_4)_3$ could be considered from $[Na_3V_2(PO_4)_3]_2$ (all ions occupations are 0.75) to $[Na_2V_2(PO_4)_3]_2$ (all ions occupations are 0.5) then to $[NaV_2(PO_4)_3]_2$, which could be utilized to account for the theoretical ion-extraction number reasonably.

4. Conclusion

A development of carbothermal reduction method based on molecular mixing in a solution called S-CTR method was used to prepare $Na_3V_2(PO_4)_3$ (NVP), and the sodium-ion battery constructed with S-CTR NVP cathode exhibited well in C-rate and cycling performances with a specific capacity of 117.6 mAhg^{-1}. Notably, the open three-dimensional framework of NASICON-type NVP has two kinds of Na sites and as reported, of which the ions extracted from Na(2) sites would be responsible for the exhibited capacity as well as the chemical diffusion with a magnitude of 10^{-11} cm^2/s. Moreover, it is suggested that the ion occupation of 0.75 for all Na sites is suitable for the configuration of $[Na_3V_2(PO_4)_3]_2$, and the two-step extraction accompanied with structural reorganization is capable to account for the theoretical capacity of $Na_3V_2(PO_4)_3$ when two ions extract from $Na_3V_2(PO_4)_3$ producing a value of 117.6 mAhg^{-1}. To the best of our knowledge, it is the first time to explore the ion-extraction number from NVP by analyzing the ions occupations.

Acknowledgements

Notes and references

College of Chemistry and Chemical Engineering, Central South University, Changsha, 410083, China. Fax: (+86)731 88879616;E-mail:xji@csu.edu.cn

1. J. M. Tarascon and M. Armand, *Nature*, 2001, **414**, 359-367.
2. M. Armand and J. M. Tarascon, *Nature*, 2008, **451**, 652-657.
3. Z. Yang, J. Zhang, M. C. W. Kintner-Meyer, X. Lu, D. Choi, J. P. Lemmon and J. Liu, *Chem. Rev.*, 2011, **111**, 3577-3613.
4. K. Saravanan, C. W. Mason, A. Rudola, K. H. Wong and P. Balaya, *Adv. Energy Mater.*, 2013, **3**, 444-450.
5. S.-W. Kim, D.-H. Seo, X. Ma, G. Ceder and K. Kang, *Adv. Energy Mater.*, 2012, **2**, 710-721.
6. J. Gopalakrishnan and K. K. Rangan, *Chem. Mater.*, 1992, **4**, 745-747.
7. B. L. Cushing and J. B. Goodenough, *J. Solid State Chem.*, 2001, **162**, 176-181.
8. H. Kabbour, D. Coillot, M. Colmont, C. Masquelier and O. Mentre, *J. Am. Chem. Soc.*, 2011, **133**, 11900-11903.
9. J. Kang, S. Baek, V. Mathew, J. Gim, J. Song, H. Park, E. Chae, A. K. Rai and J. Kim, *J. Mater. Chem.*, 2012, **22**, 20857-20860.
10. Z. Jian, W. Han, X. Lu, H. Yang, Y.-S. Hu, J. Zhou, Z. Zhou, J. Li, W. Chen, D. Chen and L. Chen, *Adv. Energy Mater.*, **3**, 156-160.
11. W. Song, X. Ji, Y. Yao, H. Zhu, Q. Chen, Q. Sun and C. E. Banks, *Phys Chem Chem Phys*, 2014, **16**, 3055-3061.
12. W. Song, X. Ji, Z. Wu, Y. Zhu, Y. Yao, K. Huangfu, Q. Chen and C. E. Banks, *ChemElectroChem*, 2014, **DOI: 10.1002/celc.201300248**.
13. W. Song, X. Ji, Z. Wu, Y. Zhu, Y. Yang, J. Chen, M. Jing, F. Li and C. E. Banks, *J. Mater. Chem. A*, 2014, **2**, 5358-5362.
14. R. A. Shakoor, D.-H. Seo, H. Kim, Y.-U. Park, J. Kim, S.-W. Kim, H. Gwon, S. Lee and K. Kang, *J. Mater. Chem.*, 2012, **22**, 20535-20541.
15. W. Song and S. Liu, *Solid State Sci.*, 2013, **15**, 1-6.
16. W. Song, X. Ji, Z. Wu, Y. Yang, Z. Zhou, F. Li, Q. Chen and C. E. Banks, *J. Power Sources*, 2014, **256**, 258-263.
17. M. D. Slater, D. Kim, E. Lee and C. S. Johnson, *Adv. Funct. Mater.*, 2013, **23**, 947-985.
18. F. Cheng, J. Liang, Z. Tao and J. Chen, *Adv. Mater.*, 2011, **23**, 1695-1715.
19. H.-K. Song, K. T. Lee, M. G. Kim, L. F. Nazar and J. Cho, *Adv. Funct. Mater.*, 2010, **20**, 3818-3834.
20. Y. Liu, Y. Xu, X. Han, C. Pellegrinelli, Y. Zhu, H. Zhu, J. Wan, A. C. Chung, O. Vaaland, C. Wang and L. Hu, *Nano Lett.*, 2012, **12**, 5664-5668.
21. Y. Zhu, Y. Xu, Y. Liu, C. Luo and C. Wang, *Nanoscale*, 2013, **5**, 780.
22. Y. Liao, K.-S. Park, P. Xiao, G. Henkelman, W. Li and J. B. Goodenough, *Chem. Mater.*, 2013, **25**, 1699-1705.
23. K. T. Lee, T. N. Ramesh, F. Nan, G. Botton and L. F. Nazar, *Chem. Mater.*, 2011, **23**, 3593-3600.
24. S. Komaba, C. Takei, T. Nakayama, A. Ogata and N. Yabuuchi, *Electrochem. Commun.*, 2010, **12**, 355-358.

25. S. Komaba, W. Murata, T. Ishikawa, N. Yabuuchi, T. Ozeki, T. Nakayama, A. Ogata, K. Gotoh and K. Fujiwara, *Adv. Funct. Mater.*, 2011, **21**, 3859-3867.

26. D. Kim, S.-H. Kang, M. Slater, S. Rood, J. T. Vaughey, N. Karan, M. Balasubramanian and C. S. Johnson, *Adv. Energy Mater.*, 2011, **1**, 333-336.

27. S. Tepavcevic, H. Xiong, V. R. Stamenkovic, X. Zuo, M. Balasubramanian, V. B. Prakapenka, C. S. Johnson and T. Rajh, *ACS Nano*, 2011, **6**, 530-538.

28. V. Palomares, M. Casas-Cabanas, E. Castillo-Martinez, M. H. Han and T. Rojo, *Energy Environ. Sci.*, 2013, **6**, 2312-2337.

29. S. Y. Lim, H. Kim, R. A. Shakoor, Y. Jung and J. W. Choi, *J. Electrochem. Soc.*, 2012, **159**, A1393-A1397.

30. W. Song, X. Ji, C. Pan, Y. Zhu, Q. Chen and C. E. Banks, *Phys Chem Chem Phys*, 2013, **15**, 14357-14363.

31. K. Du, H. Guo, G. Hu, Z. Peng and Y. Cao, *J. Power Sources*, 2013, **223**, 284-288.

32. Z. Chen, C. Dai, G. Wu, M. Nelson, X. Hu, R. Zhang, J. Liu and J. Xia, *Electrochim. Acta*, 2010, **55**, 8595-8599.

33. Z. Jian, L. Zhao, H. Pan, Y.-S. Hu, H. Li, W. Chen and L. Chen, *Electrochem. Commun.*, 2012, **14**, 86-89.

34. W. Song, X. Ji, Z. Wu, Y. Zhu, Y. Yao, K. Huangfu, Q. Chen and C. E. Banks, *J. Mater. Chem. A*, 2014, **2**, 2571-2577.

35. X. H. Rui, N. Ding, J. Liu, C. Li and C. H. Chen, *Electrochim. Acta*, 2010, **55**, 2384-2390.

36. W. Song, X. Ji, Z. Wu, Y. Zhu, F. Li, Y. Yao and C. E. Banks, *RSC Advances*, 2014, **4**, 11375-11383.